# Breast-specific gamma camera imaging with $^{99m}$Tc-MIBI has better diagnostic performance than magnetic resonance imaging in breast cancer patients: A meta-analysis

**Aimi Zhang, MD,**
**Panli Li, MD,**
**Qiufang Liu, MD,**
**Shaoli Song, MD PhD**

*Department of Nuclear Medicine, Ren Ji Hospital, School of Medicine, Shanghai Jiao Tong University.*

*Keywords:* Specific gamma imaging, -Magnetic resonance imaging, -Breast cancer, -Meta-analysis

***Corresponding author:***
Shaoli Song, MD PhD,
Associate Chief Physician
Department of Nuclear Medicine,
Ren Ji Hospital, School of Medicine,
Shanghai Jiao, Tong University,
Shanghai China, 200127.
Phone: 86- 021-68383530.
haoli-song@163.com

*Received:*
19 November 2016
*Accepted revised :*
23 December 2016

## Abstract

**Objective:** This study aimed to evaluate the diagnostic role of breast-specific gamma camera imaging (BSGI) with technetium-99m-methoxy isobutyl isonitrile ($^{99m}$Tc-MIBI) and magnetic resonance imaging (MRI) in patients with breast cancer through a meta-analysis. **Subjects and Methods:** Three reviewers searched articles published in medical journals before June 2016 in MEDLINE, EMBASE and Springer Databases; the references listed in original articles were also retrieved. We used the quality assessment of diagnostic accuracy studies (QUADAS) tool to assess the quality of the included studies. Heterogeneity, pooled sensitivity and specificity, positive likelihood ratio, negative likelihood ratio, diagnostic odds ratio (DOR) and summary receiver operating characteristic (SROC) curves were calculated by Meta-DiSc software to estimate the diagnostic performance of BSGI and MRI. Ten studies with 517 patients were included after meeting the inclusion criteria. We did a subgroup analysis of the same data type. **Results:** The pooled sensitivities of BSGI and MRI were: 0.84 (95% CI, 0.79-0.88) and 0.89 (95% CI, 0.84-0.92) respectively, and the pooled specificities of BSGI and MRI were: 0.82 (95% CI, 0.74-0.88) and 0.39 (95% CI, 0.30-0.49) respectively. The areas under the SROC curve of BSGI and MRI were 0.93 and 0.72 respectively. **Conclusion:** The results of our meta-analysis indicated that compared with MRI, BSGI has similar sensitivity, higher specificity, better diagnostic performance, and can be widely used in clinical practice.

*Hell J Nucl Med 2017; 20(1): 26-35* *Epub ahead of print: 20 March 2017* *Published online: 20 April 2017*

## Introduction

Breast cancer is the most frequently diagnosed cancer and the leading cause of cancer death in females, worldwide [1]. Mammography is a common method for screening breast cancer due to its high sensitivity, and ultrasound of the breast has been approved as an adjunct to mammography for women with dense breasts [2, 3]. However, some small and subtle breast lesions cannot be detected by mammography or ultrasound. For these lesions, magnetic resonance imaging (MRI) has a comparatively higher sensitivity [4]. Especially, contrast-enhanced MRI, can better depict the location and size of lesions and evaluate lymph node metastatic lesions not only on cross-section morphology but also on functional characteristics [5].

In recent years, as a non-invasive imaging modality and a kind of functional breast imaging technique, breast-specific gamma imaging (BSGI) with intravenous injection of technetium-99m-methoxy isobutyl isonitrile (MIBI) is increasingly used for diagnosis of breast cancer in clinical practice while its sensitivity is not influenced by breast density [6]. Breast-specific gamma imaging, also called molecular breast imaging, is a nuclear medicine breast imaging technique that uses a high resolution, small field-of-view breast-specific gamma camera [28]. Its radiotracer $^{99m}$Tc-MIBI diffuses from the blood and mostly gathers in mitochondria. Uptake and retention of $^{99m}$Tc-MIBI can reveal the level of tissue metabolism [30]. Compared with single photon emission tomography (SPET), BSGI offers superior intrinsic spatial resolution and can obtain standard mammographic views (craniocaudal [CC] and mediolateral oblique [MLO]) [7, 8]. Sensitivities and specificities of BSGI for the detection of breast cancer have been previously reported [6, 9-13].

Although there are many separate studies on BSGI and MRI, head-to-head comparison between these techniques has been rarely reported and includes only a few cases [21, 23-26]. Therefore, we conducted this meta-analysis to evaluate the diagnostic value of BSGI and MRI in the newly diagnosed or in the postoperative breast cancer patients.

## Methods

### Literature search strategy

We identified the published studies of the role of BSGI and MRI in the diagnosis of breast cancer in original articles by systematic searches of PubMed (including MEDLINE compiled by the United States National Library of Medicine, Bethesda, Maryland, USA) by using medical subject heading (MeSH) terms explicitly, Embase (Elsevier, Amsterdam, Netherlands), and Springer (Springer Science+Business Media, Berlin, Germany). The investigation was limited to studies conducted before June 2016. The keywords used were "Magnetic resonance imaging" or "MRI", "BSGI" or "Breast-specific gamma imaging" or "gamma imaging" and "Breast neoplasms or breast cancer or breast carcinoma".

### Inclusion and exclusion criteria

Three reviewers independently screened titles and abstracts to select potentially eligible articles and manually searched reference lists of retrieved studies. Then we got the full text of the articles and determined their eligibility. Articles were included if they met the following criteria: a) Patients should have been examined both by BSGI and MRI before surgery; b) At least 10 patients were included in each study; c) Studies needed sufficient information for the calculation of sensitivity, specificity, and diagnostic accuracy; d) Reference standard should be completed, such as pathological examination or clinical and imaging follow-up; e) The images of BSGI and MRI should be visually interpreted by 2 experienced specialists. Exclusion criteria were as follows: a) Papers were reviews, conference abstracts, case report, letters, editorials or comments; b) Non-human studies; c) Non-English articles; d) Studies with duplicated data; e) Unpublished articles.

### Quality assessment of the studies

Two authors independently assessed the risk of bias using the quality assessment of diagnostic accuracy studies (QUADAS) tool, which is a quality assessment tool specifically developed for systematic reviews of diagnostic accuracy studies. Fourteen items were included in the tool, covered the patient spectrum, reference standard, disease progression bias, verification bias, review bias, clinical review bias, incorporation bias, test execution, study withdrawals, and indeterminate results [14]. According to the guidelines, each of the items was scored to clarify studies as having high (yes), low (no) or unclear quality (unclear). The BSGI and MRI tests of each study were evaluated separately. The number of items evaluated as "yes" were regarded as QUADAS score of each study.

### Data extraction

Two reviewers extracted data independently using a predefined data extraction form and any disagreements were resolved by discussion. The data extracted included the first author, study characteristics (i.e., country, year, and study design), patient characteristics (i.e., mean age, sample size, and patient/lesion based), subgroup information (histologic and molecular classification), reference standard, state before examination (confirm/suspicious), injected dose of $^{99m}$Tc-MIBI, image interpretation method of BSGI and MRI, as well as scan sequence of MRI (plain or contrast, type of functional imaging). True positive (TP), false positive (FP), false negative (FN) and true negative (TN) were extracted from each article.

### Data synthesis and statistical analysis

We constructed a 2×2 contingency table for each study with results of TP, FP, FN, TN. By using these tables, pooled sensitivity and specificity, with 95% confidence intervals (CI), of two index tests of included studies were calculated, to compare the diagnostic accuracy of the two imaging modalities. A value of 1/2 was added to all empty cells or of studies to avoid potential problems in the calculation of summary estimates. Five studies only took pathology-proven patients into consideration. Therefore, the specificity of these studies was not reported and the FP and TN rates were recorded as 0.5. Positive likelihood ratio ($LR^+$), negative likelihood ratio (LR-), diagnostic odds ratio (DOR) and summary receiver operating characteristic (SROC) curves were also calculated. The area under the curve (AUC) of the SROC was also used as an indicator of the performance of BSGI and MRI.

We used likelihood ratio $I^2$ index and $\chi^2$ test (Chi-squared test or Q test) to assess heterogeneity. $I^2$ index is a measure of the percentage of total variation across studies due to heterogeneity beyond chance; a value over 50% indicates heterogeneity [15]. Regarding $\chi^2$ test, when the p-value of a Q statistic was less than 0.05, it was considered as having apparent heterogeneity. We selected the random effects model (REM) when there was heterogeneity, otherwise we used the fixed effects model (FEM). A threshold effect was one of the main causes of heterogeneity when testing accuracy. The Spearman correlation coefficients for two index tests were calculated. If $P>0.05$, there was no threshold effect [16]. We used Deeks' funnel plot to analyze the publication bias of all included studies.

All statistical analysis was completed using Meta-DiSc 1.4 (a free software to perform meta-analysis of studies of evaluations of diagnostic and screening tests) and Stata 12.0 (Stata Corporation, College Station, TX, USA).

## Results

### Study identification and selection

A total of 131 records were obtained in the initial search using the outlined search strategy. We found 16 articles considered potentially eligible and the full text was retrieved after reviewing title and abstract. Of the 16 full-text articles, 6 studies were excluded. Finally, we included 10 articles in our meta-analysis [17-26]. The flow diagram of the article selection process is presented in Figure 1.

### Study characteristics

The characteristics of included studies are shown in Table 1.

The ten studies had a total of 590 subjects, including 517 patients, aged from 24 to 82. Four studies [18, 19, 23, 24] had a patients-based data type while eight [17, 20-26] had a lesion-based data type. Therefore, we included these eight studies of the same data type (lesion-based) to do a subgroup analysis of 393 lesions. The sample size of the studies ranged from 18 to 122 and the median sample size was 59. Five studies were from the USA, 4 from Korea and 1 from Austria. Among the 10 included publications, 7 were retrospective while 3 were prospective. Eight studies [19-26] reported histologic classification and 3 [19, 22, 24] reported molecular typing. All studies chose biopsy or postoperative pathology as the reference standard. Some studies have evaluated diagnostic value of mammography or ultrasound in patients with breast cancer, but we only extracted BSGI and MRI data. Among 10 included studies, 5 studies [22-26] lacked data of specificity because the study subjects initially selected were patients diagnosed with breast cancer by gold standard. Finally, only 3 studies [17, 20, 21] were available in the calculation of the pooled specificity according to lesions. Other details including imaging protocols and the diagnostic performance of each study are shown in Table 2.

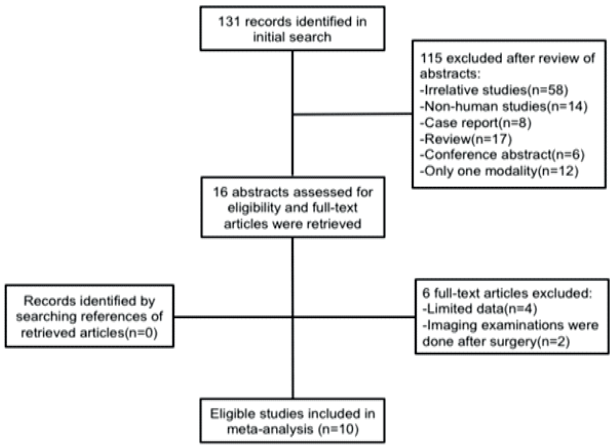


**Figure 1.** Flow chart of study selection process for meta-analysis.

## Quality assessment

We used QUADAS tool to assess the studies included and the results of BSGI and MRI are reported separately. The QUADAS scores of each study are shown in Table 1. The quality assessment items and the likelihood of bias are summarized in Figure 2 and Figure 3. The reasons for unsatisfactory accordance of the representative spectrum (40% [17, 18, 21, 26]) were that half of the studies selected pathologically confirmed patients as subjects and that most studies were done in local institutions, resulting in a narrow spectrum of patients. The item of reference standard blinded was mostly reported unclearly, because most articles failed to provide specific execution of gold standard. On the whole, the qualities of the included studies were satisfactory and qualified.

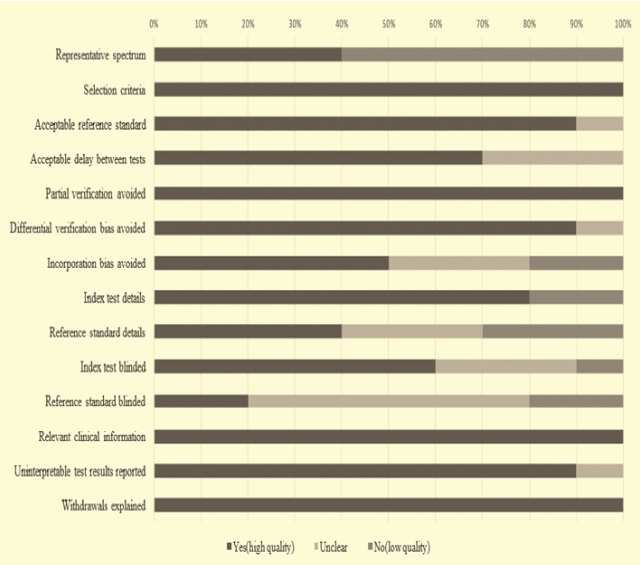


**Figure 2.** Methodological quality of included studies for BSGI according to the Quality Assessment of Diagnostic Accuracy Studies (QUADAS) tool.

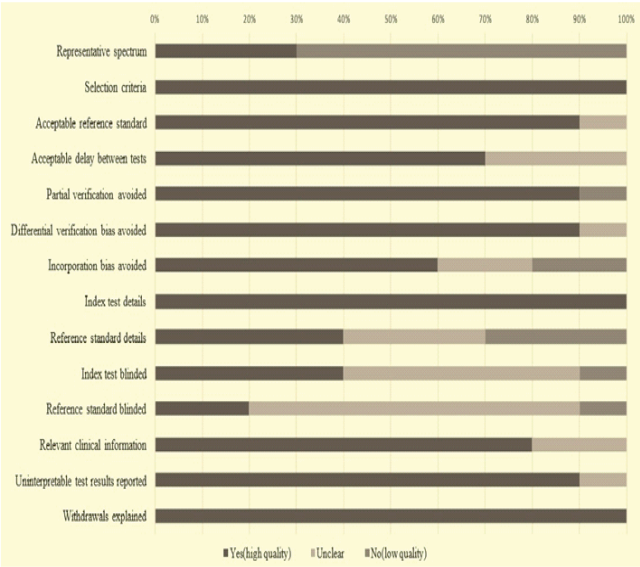


**Figure 3.** Methodological quality of included studies for MRI according to the Quality Assessment of Diagnostic Accuracy Studies (QUADAS) tool.

## Heterogeneity test and publication bias

The heterogeneity test indicated statistical heterogeneity for two imaging modalities among studies, so we chose random effects model to calculate the pooled estimates. The statistical heterogeneity of BSGI and MRI are displayed in Figure 4 (sensitivity, Q value=9.1 $I^2$=22.3%; specificity, Q value=8.30, I2=75.9%) and Figure 5 (sensitivity, Q value= 9.42 $I^2$=25.7%; specificity, Q value=4.12, $I^2$=51.4%). The $I^2$ index can assess not only heterogeneity but also the degree of that heterogeneity as low (25%), moderate (50%), and high (75%) [26]. The Spearman correlation coefficient and P value of BSGI and MRI were 0.082 (P=0.846, P>0.05) and 0.709 (P=0.049, P<0.05), respectively. The result of MRI showed the existence of threshold effects in this meta-analysis. Deeks' Funnel plots of the included studies are presented in Figure 6, which showed insignificant publication bias (P=0.16, 0.61, respectively).

**Table 1.** *Characteristics of the 10 studies included in the meta-analysis.*

| Author | Country | Year | Study design | Sample size | Patients/ Lesions | Median age (year) | Histologic subtype | Molecular subtype | Reference standard | QDAS score |
|---|---|---|---|---|---|---|---|---|---|---|
| Meissnitzer et al[17] | Austria | 2015 | Pro | 92 | Lesions | >50 | Benign(25) DCIS(3) IDC(53) Others(11) | NR | Biopsy | 11(BSGI) |
| Johnson et al[18] | USA | 2014 | Retro | 75 | Patients | NR | NR | NR | Biopsy | 8(BSGI) 6(MRI) |
| Lee et al[19] | Korea | 2014 | Retro | 122 | Pateints | 45.9(29-71) | IDC(115) Others(7) | ER+(65) PR+(49) HER2+(38) | Postoperative pathology | 12(BSGI) 11(MRI) |
| Kim et al[20] | Korea | 2012 | Retro | 97 | Lesions | 44.1 | Benign(71) DCIS(6) IDC(16) Others(4) | NR | Biopsy | 9(BSGI) 9(MRI) |
| Brem et al[21] | USA | 2007 | Pro | 33 | Lesions | 53(33-70) | Benign(24) DCIS(4) IDC(3) ILC(1) Others(1) | NR | Biopsy or follow-up | 10(BSGI) 10(MRI) |
| Yoon et al[22] | Korea | 2015 | Retro | 68 | Lesions | 49.5(24-73) | DCIS(58) IDC(10) | ER+(49) PR+(53) HER2+(26) | Biopsy and postoperative pathology | 13(BSGI) 10(MRI) |
| Kim et al[23] | Korea | 2014 | Retro | 35 | Patients& lesions | 48(26-69) | DCIS(35) | NR | Biopsy and postoperative pathology | 10(BSGI) 10(MRI) |
| Keto et al[24] | USA | 2012 | Pro | 18 | Patients& lesions | 51 | DCIS(18) | ER+(16) PR+(12) | NR | 8(BSGI) 8(MRI) |
| Brem et al[25] | USA | 2009 | Retro | 28 | Lesions | 62.8(46-82) | ILC(28) | NR | Biopsy and postoperative pathology | 9(BSGI) 8(MRI) |
| Brem et al[26] | USA | 2007 | Retro | 22 | Lesions | 55(34-76) | DCIS(22) | NR | Biopsy and postoperative pathology | 10(BSGI) 9(MRI) |

*(Pro, prospective; Retro, retrospective; NR, not reported; DCIS, ductal carcinoma in situ; IDC, invasive ductal carcinoma ILC, invasive lobular carcinoma)*

*Table 2. Imaging protocols and diagnostic performance of two image modalities.*

| Author | Country | Year | Image | State before examination | Image interpretation method | Injected dose of $^{99m}$Tc-MIBI (MBq) | MRI sequence and functional MRI | Sensitivity | Specificity |
|---|---|---|---|---|---|---|---|---|---|
| Meissnitzer et al[17] | Austria | 2015 | BSGI | Suspicious | Visual and semi-quantitative | 740-1110 | | 0.90 | 0.56 |
| | | | MRI | >> | Visual | | DCE-MRI, fat-suppressed T2, DWI | 0.88 | 0.40 |
| Johnson et al[18] | USA | 2014 | BSGI | >> | >> | 925-1110 | | 0.92 | 0.73 |
| | | | MRI | >> | NR | | Unclear | 0.89 | 0.54 |
| Lee et al[19] | Korea | 2014 | BSGI | >> | Visual | 925-1110 | | 0.740 | 0.722 |
| | | | MRI | >> | NR | | DCE-MRI | 0.817 | 0.722 |
| Kim et al[20] | Korea | 2012 | BSGI | Confirmed | Visual | 740 | | 0.888 | 0.901 |
| | | | MRI | >> | >> | | DCE-MRI, fat-suppressed T2, DWI | 0.923 | 0.394 |
| Brem et al[21] | USA | 2007 | BSGI | Suspicious | >> | 925-1110 | | 0.89 | 0.71 |
| | | | MRI | >> | >> | | DCE-MRI | 1.00 | 0.25 |
| Yoon et al[22] | Korea | 2015 | BSGI | Confirmed | Visual and quantitative | 555-925 | | 0.83 | NR |
| | | | MRI | >> | NR | | DCE-MRI, fat-suppressed T2, DWI, ADC-MRI | 0.94 | NR |
| Kim et al[23] | Korea | 2014 | BGI | >> | Visual | 925-1110 | | 0.686 | NR |
| | | | MRI | >> | >> | | DCE-MRI | 0.914 | NR |
| Keto et al[24] | USA | 2012 | BSGI | >> | >> | 925 | | 0.89 | NR |
| | | | MRI | >> | >> | | E-MRI, MIP | 0.94 | NR |
| Brem et al[25] | USA | 2009 | BGI | >> | >> | 740-925 | | 0.93 | NR |
| | | | MRI | >> | >> | | Plain+ E-MRI, 3D volumetric imaging | 0.83 | NR |
| Brem et al[26] | USA | 2007 | BSGI | >> | >> | 925-1110 | | 0.91 | |
| | | | MRI | Confirmed | >> | | E-MRI, fat-suppressed T2, 3D volumetric dynamic imaging | 0.88 | NR |

*(DCE-MRI, dynamic contrast-enhanced MRI; E-MRI, enhanced-MRI; DWI, diffusion-weighted imaging; ADC-MRI, apparent diffusion coefficient MRI; MIP, maximum intensity projection; NR, not reported)*

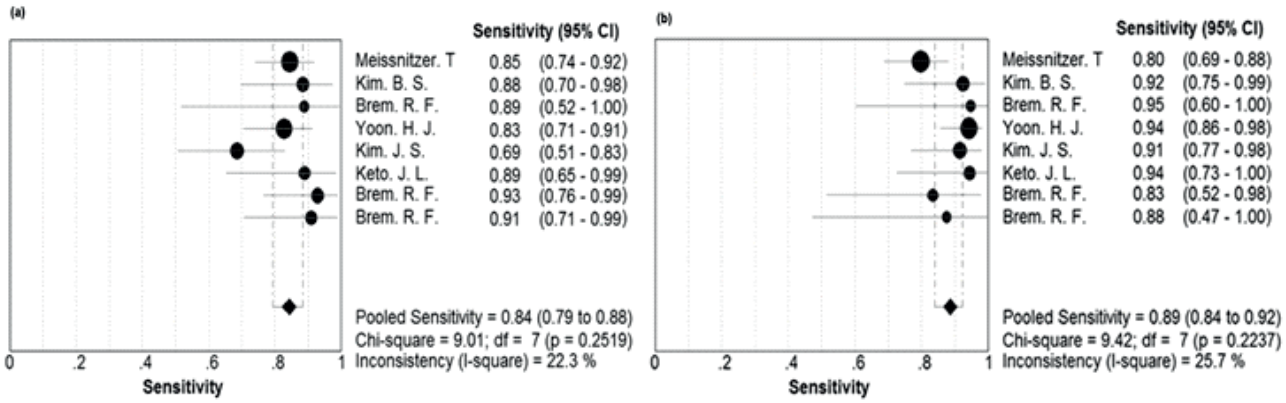


**Figure 4.** The pooled sensitivity of BSGI (a) and MRI (b). The size of the square plotting reflects the study weight. Horizontal lines are the 95% confidence intervals.

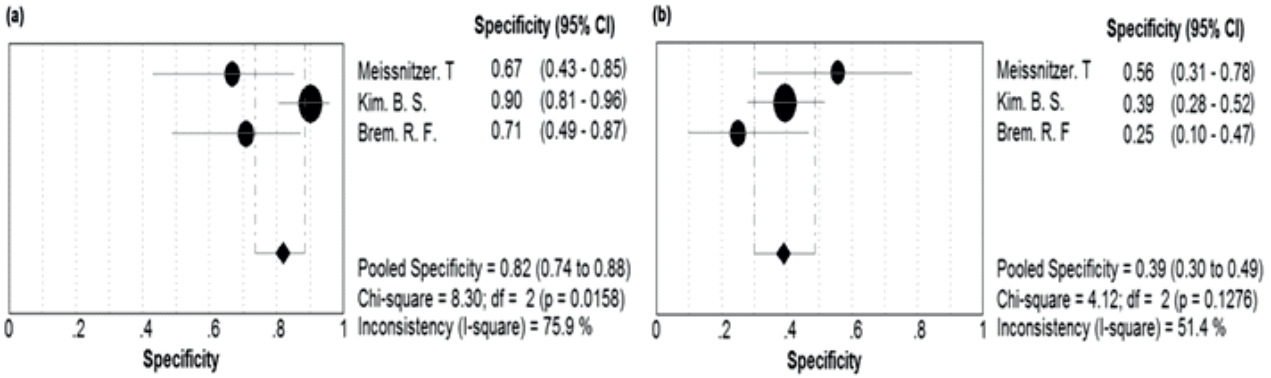


**Figure 5.** The pooled specificity of BSGI (a) and MRI (b). The size of the square plotting reflects the study weight. Horizontal lines are the 95% confidence intervals.

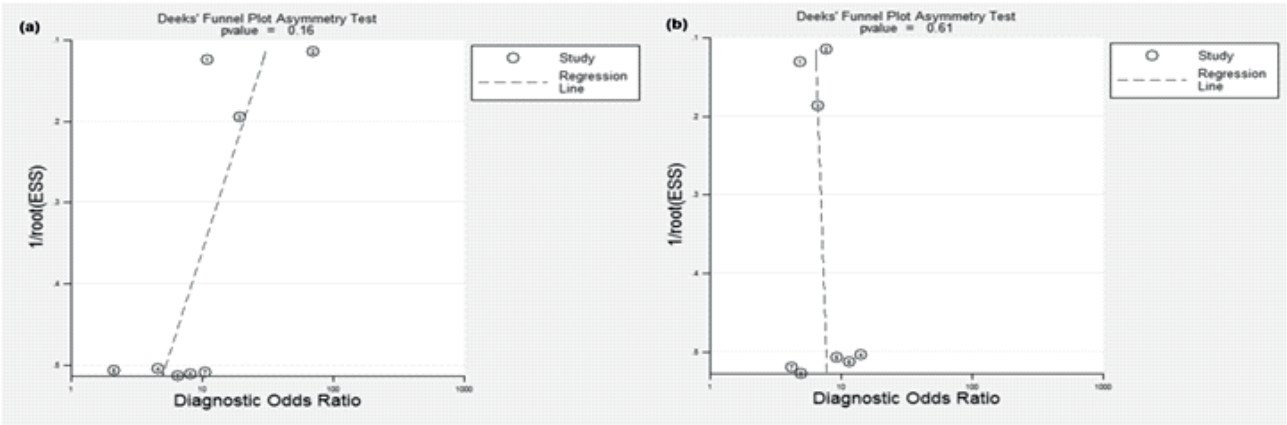


**Figure 6.** (a) Publication bias of BSGI using Deek's funnel plot. (b) Publication bias of MRI using Deek's funnel plot.

### Diagnostic accuracy of BSGI and MRI

The pooled sensitivities of BSGI and MRI were 0.84 (95% CI, 0.79-0.88) and 0.89 (95% CI, 0.84-0.92), respectively, and the pooled specificities of BSGI and MRI were 0.82 (95% CI, 0.74-0.88) and 0.39 (95% CI, 0.30-0.49), respectively (Figure 4 and Figure 5). The results indicated that the sensitivity of MRI was slightly higher than BSGI, but the specificity of BSGI was significantly higher than MRI. For BSGI, positive likelihood ratio ($LR^+$), negative likelihood ratio ($LR^-$) and diagnostic odds ratio (DOR) were 3.15 (95% CI, 1.92-5.16), 0.21 (95% CI, 0.13-0.34) and 17.56 (95% CI, 8.32-37.09), respectively, while for MIR, they were 1.46 (95% CI, 1.24-1.71), 0.29 (95% CI, 0.18-0.47) and 6.34 (95% CI, 2.92-13.75), respectively (Figure 7 and Figure 8). Summary received operating characteristics curves of BSGI and MRI were presented in Figure 9, the AUC values of which were 0.93 and 0.72, respectively, indicating a higher diagnostic accuracy of BSGI. The above results of this meta-analysis are presented in Table 3.

## Discussion

***Table 3.*** *The overall diagnostic value of two image modalities.*

| Result | Sensitivity (95%CI) | Specificity (95%CI) | DOR | AUC | $LR^+$ | $LR^-$ |
|---|---|---|---|---|---|---|
| BSGI | 0.84 | 0.82 | 17.56 | 0.93 | 3.15 | 0.21 |
| | (0.79 -0.88) | (0.74 - 0.88) | (8.32 - 37.09) | | (1.92 - 5.16) | (0.13 - 0.34) |
| MRI | 0.89 | 0.39 | 6.34 | 0.72 | 1.46 | 0.29 |
| | (0.84 - 0.92) | (0.30 - 0.49) | (2.92 - 13.75) | | (1.24 - 1.71) | (0.18 - 0.47) |

*(CI, confidence interval; DOR, diagnostic odds ratio; AUC, area under the curve; $LR^+$, positive likelihood ratio; $LR^-$, negative likelihood ratio)*

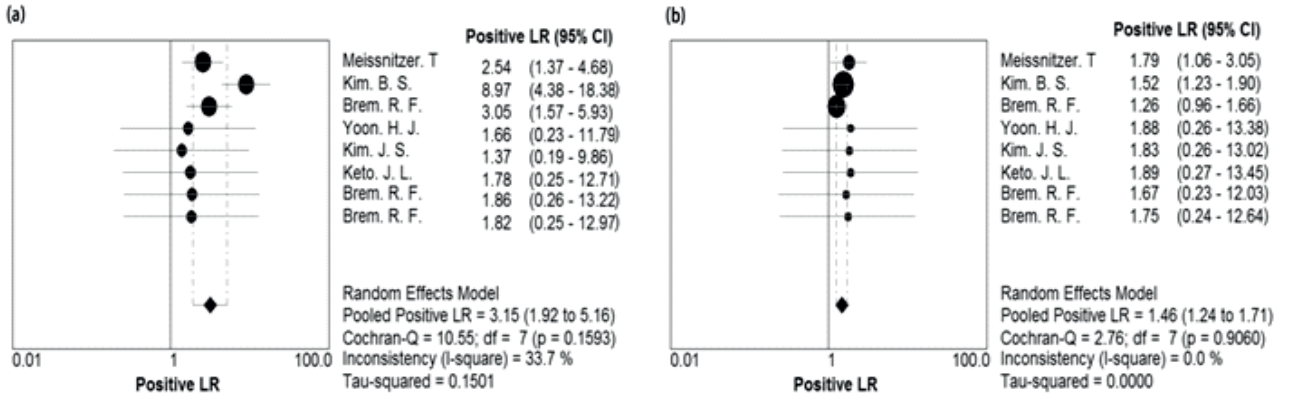


**Figure 7.** The pooled positive likelihood ratio of BSGI (a) and MRI (b). The size of the square plotting reflects the study weight. Horizontal lines are the 95% confidence intervals.

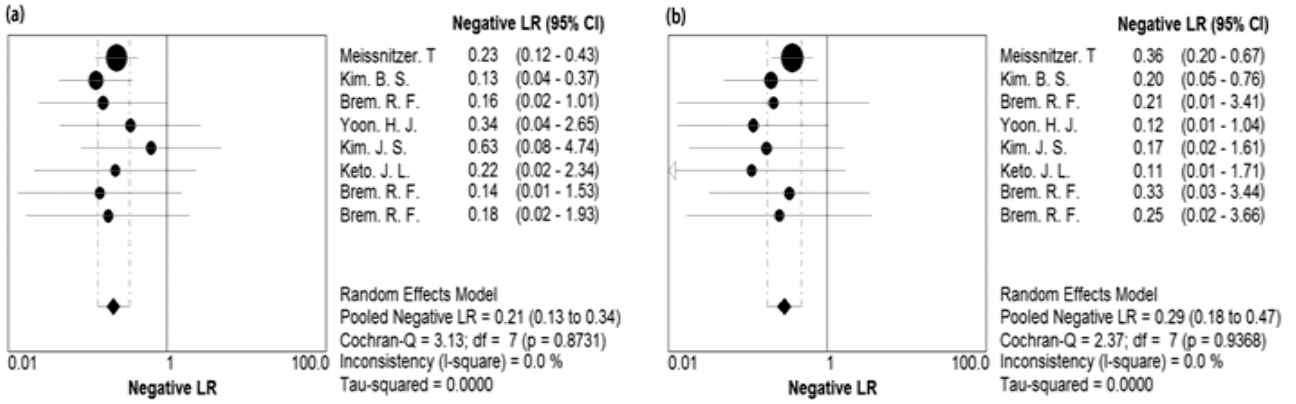


**Figure 8.** The pooled negative likelihood ratio of BSGI (a) and MRI (b). The size of the square plotting reflects the study weight. Horizontal lines are the 95% confi-dence intervals.

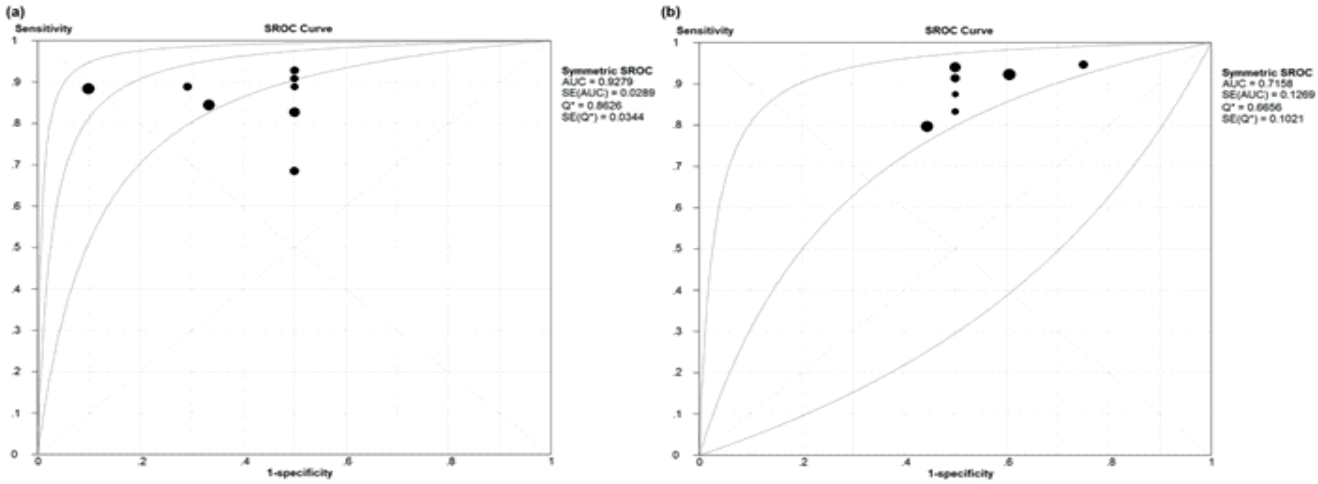


**Figure 9.** The pooled negative likelihood ratio of BSGI (a) and MRI (b). The size of the square plotting reflects the study weight. Horizontal lines are the 95% confi-dence intervals.

For diagnosis of breast cancer, Breast specific gamma imaging, as a new functional imaging modality, is increasingly used in clinical practice, while MRI, especially enhanced-MRI, is regarded as a routine method to make up for the limitations of mammography and ultrasound. Previous meta-analyses have suggested that BSGI had a high diagnostic performance as an excellent adjunct modality to mammography or ultrasound for detecting breast cancer [28] and MRI of the breast has high sensitivity and lower specificity in the evaluation of breast lesions [29]. In our study, pooled estimates and SROC curves were obtained to compare BSGI with MRI in detecting breast lesions. To our knowledge, this is the first meta-analysis to compare these two imaging modalities in patients with breast cancer.

In this study, we systematically evaluated the diagnostic value of BSGI and MRI in the same cohort patients with breast cancer. The results of the meta-analysis showed that compared with MRI, BSGI had sensitivity on par with MRI (84% vs 89%) but a higher specificity (82% vs 39%) and diagnostic efficacy (AUC 0.93 vs 0.72), indicating an excellent diagnostic performance.

The overall $LR^+$ of BSGI was 3.15, and $LR^-$ was 0.21, which were slightly different with the previous meta-analysis of Yu et al. (2013) [28]. In their study, the sensitivity, specificity, $LR^+$, $LR^-$ and AUC value of BSGI were 95%, 80%, 4.63, 0.08 and 0.9552, respectively. The difference might have resulted from the characteristics of lesions in included studies, like histopathological type and molecular type of cancers, which might reduce the sensitivity. Brem et al. (2007, 2009) [25, 26] reported that the sensitivity of BSGI in detecting invasive lobular carcinoma (ILC) was 93% while for ductal carcinoma in situ (DCIS) was 91%. Five studies [22-26] in our meta-analysis selected patients with lesions of a single pathological type as study objects, which may have contributed to the difference. Histopathological subgroup analysis cannot be performed due to limitations of the number of studies and information insufficiency of each study.

In all included studies, BSGI used $^{99m}$Tc-MIBI as radiotracer. As a non-specific tracer, $^{99m}$Tc-MIBI diffuses from the blood into the cytoplasm, and 90% gathers in mitochondria. Uptake and retention of $^{99m}$Tc-MIBI depend on angiogenesis and regional perfusion, plasma and mitochondrial membrane potentials and thus the level of tissue metabolism [30]. Thus compared with the surrounding normal tissue, there is a higher uptake of $^{99m}$Tc-MIBI in the cancer cells [31]. But breast benign hyperplasia lesions like fibrocystic change and fibroadenoma can also cause FP results in BSGI. False negative results appeared in some poorly-differentiated DCIS [21, 22, 26]. Heudel et al. [32] also found that uptake of $^{99m}$Tc-MIBI in the 11 cases with lobular and tubulolobular carcinomas was lower than that in the ductal types. Some small lesions, especially sub-centimeter ones, could also cause FN. In the report of Meissnitzer et al. (2015), the sensitivity of BSGI for lesions <1 cm declined significantly to 60% [17].

Our results of MRI in the meta-analysis were comparable to those of Meissnitzer et al. (2015) [17] (sensitivity: 89% vs 88%, specificity: 39% vs 40%). On the whole, our results were concordant with theirs, but the application of different MR sequences may influence the results. All included studies reported the application of enhanced-MRI except one [18], whose results had no significant effect on the overall results according to a sensitivity analysis. Three studies used DWI sequence [17, 20, 22] (Table 2), which is effective in distinguishing malignant and benign breast lesions with analysis of quantitative apparent diffusion coefficient (ADC) values [33]. Other MR techniques can also play important roles in the diagnosis of breast cancer, like fat-suppressed imaging, contrast-enhanced dynamic, maximum intensity projection (MIP) and sensitivity-encoding sense [34-36]. However, some benign hyperplasia lesions, micro enhanced lesions during the menstrual phase and local inflammation or necrosis after surgery or radiotherapy can cause FP results in MRI.

In addition to high specificity, which can help reduce numbers of biopsies of benign lesions, BSGI has the other advantages in the diagnosis of breast cancer: firstly, since Chinese women usually have smaller and denser breasts [40], the images of BSGI are not influenced by density and size of breasts. It is also relatively sensitive for small lesions and occult foci. Secondly, compared with MRI, some contraindications can be avoided, such as gadolinium allergies, claustrophobia, pacemaker and other metal implants. Instead of a prone position of MRI, BSGI obtains images in an upright seated position so the patients will be more comfortable. Furthermore, mediolateral oblique (MLO) views, as well as craniocaudal (CC) views allow a direct comparison to mammogram images. Thirdly, BSGI is more economical and efficient than MRI. Compared with hundreds of images obtained with MRI, only four to ten images are obtained with BSGI, the interpretation time of which is shorter as well. Zhou et al. (2008) [37] reported the total costs of BSGI and MRI in their institutions were $1,259, $3,400, respectively; Johnson et al. (2015) [18] reported institutional charges for BSGI and MRI were $850 and $3,381, respectively. Furthermore, BSGI is superior to MRI in the assessment of the response to neoadjuvant chemotherapy [19, 38] and is valuable for the preoperative evaluation of the extent of lesions. It can also help in the selection of a target for biopsy in the case of more than one lesion [17].

However, in detecting smaller lesions, morphological imaging modalities like MRI are superior to BSGI owing to a higher spatial resolution [17]. Breast specific gamma imaging also has limitations in detecting axillary lymph nodes and delineating adjacent lesions. In addition to these, we should not overlook radiation issue of $^{99m}$Tc-MIBI. The injected dose of $^{99m}$Tc-MIBI ranged from 555-1110MBq in all included studies (Table 2). Approximately 740–1110MBq of $^{99m}$Tc-MIBI are recommended, and the effective dose equivalent for BSGI study is about 6.29–9.44mSv, which is relatively high compared with 0.7–1.0mSv of a screening mammogram [20]. There is a trend towards the application of BSGI in a low dose of $^{99m}$Tc-MIBI in the future. Hruska et al. (2012) [39] have tried two methods to reduce dose: collimators opti-mized and widened energy acceptance window. They found that administered doses of 296MBq $^{99m}$Tc-MIBI with the applied count sensitivity improvements permitted the detection of small breast lesions in patients. Their findings suggested that further reductions in acquisition duration or administered dose may be available [39]. More studies are needed for its clinical application.

Some limitations in our meta-analysis should be mentioned. First, some relevant articles might have been omitted even though we tried our best to retrieve medical literature. Second, there is not enough work on BSGI, as is a relatively new modality and is not widely used in clinical practice; therefore, the number of included studies is small and more ideal data types are needed. Some causes to heterogeneity or bias can hardly be avoided, due to the limited number of studies. Third, several factors may contribute to the heterogeneity; for example, seven studies were retrospective, except for three prospective studies with small sample sizes; studies included varied in image protocols and interpretation, methods of reference standard and ability of radiologists; among ten studies, five were from the US, four from Korea and only one from Europe, and three studies had the same Author. Unfortunately, it is difficult for us to find the exact source of heterogeneity due to the limited information.

Further studies on the role of BSGI in breast cancer are needed in the future, from lesion screening to evaluation of response to chemotherapy. We also need a larger sample for subgroup analyses, including different pathological subtypes and molecular subtypes.

*In conclusion*, our meta-analysis indicates that compared with MRI, BSGI has similar sensitivity but higher specificity and diagnostic performance. Breast specific gamma imaging can be widely used in clinical practice not only as an adjunct modality to mammography and ultrasound in the early detection of breast cancer, but also as a valuable examination in the assessment of the response to neoadjuvant chemotherapy and in directing the operation, especially when MRI is unavailable.

*Acknowledgment*

This work was funded by the National Natural Science Foundation of China (Grants No. 81471708), and Shanghai Jiao Tong University Medical Engineering Cross research fund (No.YG2012MS13).

The *authors declare that they have no conflicts of interest*

## Bibliography

1. A Jemal, F Bray, MM Center et al. Global cancer statistics. *CA Cancer J Clin* 2011; 61(2): 69-90.
2. Berry DA, Cronin KA, Plevritis SK et al. Effect of screening and adjuvant therapy on mortality from breast cancer. *N Engl J Med* 2005; 353(17): 1784-92.
3. Giger ML, Karssemeijer N, Schnabel JA. Breast image analysis for risk assessment, detection, diagnosis, and treatment of cancer. *Annu Rev Biomed Eng* 2013; 15: 327-57.
4. Houssami N, Ciatto S, Macaskill P et al. Accuracy and surgical impact of magnetic resonance imaging in breast cancer staging: systematic review and meta-analysis in detection of multifocal and multicentric cancer. *J Clin Oncol* 2008; 26(19): 3248-58.
5. Kuhl C. The Current Status of Breast MR Imaging Part I. Choice of Technique, Image Interpretation, Diagnostic Accuracy, and Transfer to Clinical Practice 1. *Radiology* 2007; 244(2): 356-78.
6. Brem RF, Floerke AC, Rapelyea JA et al. Breast-specific gamma imaging as an adjunct imaging modality for the diagnosis of breast cancer 1. *Radiology* 2008; 247(3): 651-7.
7. Hruska CB, O'Connor MK. Quantification of lesion size, depth, and uptake using a dual-head molecular breast imaging system. *Med Phys* 2008; 35: 1365-76.
8. Hruska CB and O'Connor MK. Quantification of lesion size, depth, and uptake using a dual-head molecular breast imaging system. *Med Phys* 2008; 35(4): 1365-76.
9. Lee A, Chang J, Lim W et al. Effectiveness of Breast-Specific Gamma Imaging (BSGI) for Breast Cancer in Korea: A Comparative Study. *Breast J* 2012; 18(5): 453-8.
10. Kuhn KJ, Rapelyea JA, Torrente J et al. Comparative Diagnostic Utility of Low-Dose Breast-Specific Gamma Imaging to Current Clinical *Standard. Breast J* 2016; 22(2): 180-8.
11. Park KS, Chung HW, Yoo YB et al. Complementary role of semiquantitative analysis of breast-specific gamma imaging in the diagnosis of breast cancer. *Am J Roentgenol* 2014; 202(3): 690-5.
12. Rechtman LR, Lenihan MJ, Lieberman JH et al. Breast-specific gamma imaging for the detection of breast cancer in dense versus nondense breasts. *Am J Roentgenol* 2014; 202(2): 293-8.
13. Park JS, Lee AY, Jung KP et al. Diagnostic Performance of Breast-Specific Gamma Imaging (BSGI) for Breast Cancer: Usefulness of Dual-Phase Imaging with $^{99m}$Tc-sestamibi. *Nucl Med Mol Imaging* 2013; 47(1): 18-26.
14. Whiting P, Rutjes AWS, Reitsma JB et al. The development of QUADAS: a tool for the quality assessment of studies of diagnostic accuracy included in systematic reviews. *BMC Med Res Methodol* 2003; 3(1): 1.
15. Huedo-Medina TB, Sánchez-Meca J, Marín-Martínez F et al. Assessing heterogeneity in meta-analysis: Q statistic or $I^2$ index? *Psychol Methods* 2006; 11(2): 193.
16. Zamora J, Abraira V, Muriel A et al. Meta-DiSc: a software for meta-analysis of test accuracy data. *BMC Med Res Methodol* 2006; 6(1): 1.
17. Meissnitzer T, Seymer A, Keinrath P et al. Added value of semi-quantitative breast-specific gamma imaging in the work-up of suspicious breast lesions compared to mammography, ultrasound and 3-T MRI. *Br J Radiol* 2015; 88(1051): 20150147.
18. Johnson N, Sorenson L, Bennetts L et al. Breast-specific gamma imaging is a cost effective and efficacious imaging modality when compared with MRI. *The American Journal of Surgery* 2014; 207(5): 698-701.
19. Lee HS, Ko BS, Ahn SH et al. Diagnostic performance of breast-specific gamma imaging in the assessment of residual tumor after neoadjuvant chemotherapy in breast cancer patients. *Breast Cancer Res Treat* 2014; 145(1): 91-100.
20. Kim BS. Usefulness of breast-specific gamma imaging as an adjunct modality in breast cancer patients with dense breast: a comparative study with MRI. *Ann Nucl Med* 2012; 26(2): 131-7.
21. Brem RF, Petrovitch I, Rapelyea JA et al. Breast-specific gamma imaging with $^{99m}$Tc-Sestamibi and magnetic resonance imaging in the diagnosis of breast cancer-a comparative study. *Breast J* 2007; 13(5): 465-9.
22. Yoon HJ, Kim Y, Kim BS. Intratumoral metabolic heterogeneity predicts invasive components in breast ductal carcinoma in situ. *Eur Radiol* 2015; 25(12): 3648-58.
23. Kim JS, Lee SM, Cha ES. The diagnostic sensitivity of dynamic contrast-enhanced magnetic resonance imaging and breast-specific gamma imaging in women with calcified and non-calcified DCIS. *Acta Radiol* 2014; 55(6): 668-75.
24. Keto JL, Kirstein L, Sanchez DP et al. MRI versus breast-specific gamma imaging (BSGI) in newly diagnosed ductal cell carcinoma-in-situ: a prospective head-to-head trial. *Ann Surg Oncol* 2012; 19(1): 249-52.
25. Brem RF, Ioffe M, Rapelyea JA et al. Invasive lobular carcinoma: detection with mammography, sonography, MRI, and breast-specific gamma imaging. *Am J Roentgenol* 2009; 192(2): 379-83.
26. Brem RF, Fishman M, Rapelyea JA. Detection of Ductal Carcinoma in Situ with Mammography, Breast Specific Gamma Imaging, and Magnetic Resonance Imaging: A Comparative Study. *Acad Radiol* 2007; 14(8): 945-50.
27. Berlin JA. Invited commentary: benefits of heterogeneity in meta-analysis of data from epidemiologic studies. *Am J Epidemiol* 1995; 142(4): 383-7.
28. Sun Y, Wei W, Yang H-W et al. Clinical usefulness of breast-specific gamma imaging as an adjunct modality to mammography for diagnosis of breast cancer: a systemic review and meta-analysis. *Eur J Nucl*

*Med Mol Imaging* 2013; 40(3): 450-63.
29. Peters NHGM, Borel Rinkes IHM, Zuithoff NPA et al. Meta-analysis of MR imaging in the diagnosis of breast lesions 1. *Radiology* 2008; 246(1): 116-24.
30. Buscombe JR, Cwikla JB, Thakrar DS, Hilson AJ. Uptake of Tc-99m MIBI related to tumour size and type. *Anticancer Res* 1997; 17: 1693-4.
31. Delmon-Moingeon LI, Piwnica-Worms D, Van den Abbeele AD et al. Uptake of the cation hexakis (2-methoxyisobutylisonitrile)-technetium-99m by human carcinoma cell lines in vitro. *Cancer Res* 1990; 50(7): 2198-202.
32. Heudel P, Cimarelli S, Montella A et al. Value of PET-FDG in primary breast cancer based on histopathological and immunohistochemical prognostic factors. *Int J Clin Oncol* 2010; 15(6): 588-93.
33. Guo Y, Cai YQ, Cai ZL et al. Differentiation of clinically benign and malignant breast lesions using diffusion-weighted imaging. *J Magn Reson Imaging* 2002; 16(2): 172-8.
34. Heiberg EV, Perman WH, Herrmann VM et al. Dynamic sequential 3D gadolinium-enhanced MRI of the whole breast. *Magn Reson Imaging* 1996; 14(4): 337-48.
35. Weinreb JC, Newstead G. MR imaging of the breast. *Radiology* 1995; 196(3): 593-610.
36. Larkman DJ, deSouza NM, Bydder M et al. An investigation into the use of sensitivity-encoded techniques to increase temporal resolution in dynamic contrast-enhanced breast imaging. *J Magn Reson Imaging* 2001; 14(3): 329-35.
37. Zhou M, Johnson N, Blanchard D et al. 80Real-world application of breast-specific gamma imaging, initial experience at a community breast center and its potential impact on clinical care. *Am J Surg* 2008; 195(5): 631-5; discussion 5.
38. Spanu A, Farris A, Chessa F et al. Planar scintimammography and SPECT in neoadjuvant chemo or hormonotherapy response evaluation in locally advanced primary breast cancer. *Int J Oncol* 2008; 32(6): 1275-83.
39. Hruska CB, Weinmann AL, Skjerseth CMT et al. Proof of concept for low-dose molecular breast imaging with a dual-head CZT gamma camera. Part II. Evaluation in patients. *Med Phys* 2012; 39(6): 3476.
40. Fan L, Strasser-Weippl K, Li JJ et al. Breast cancer in China. *Lancet Oncol* 2014; 15(7): e279-89.

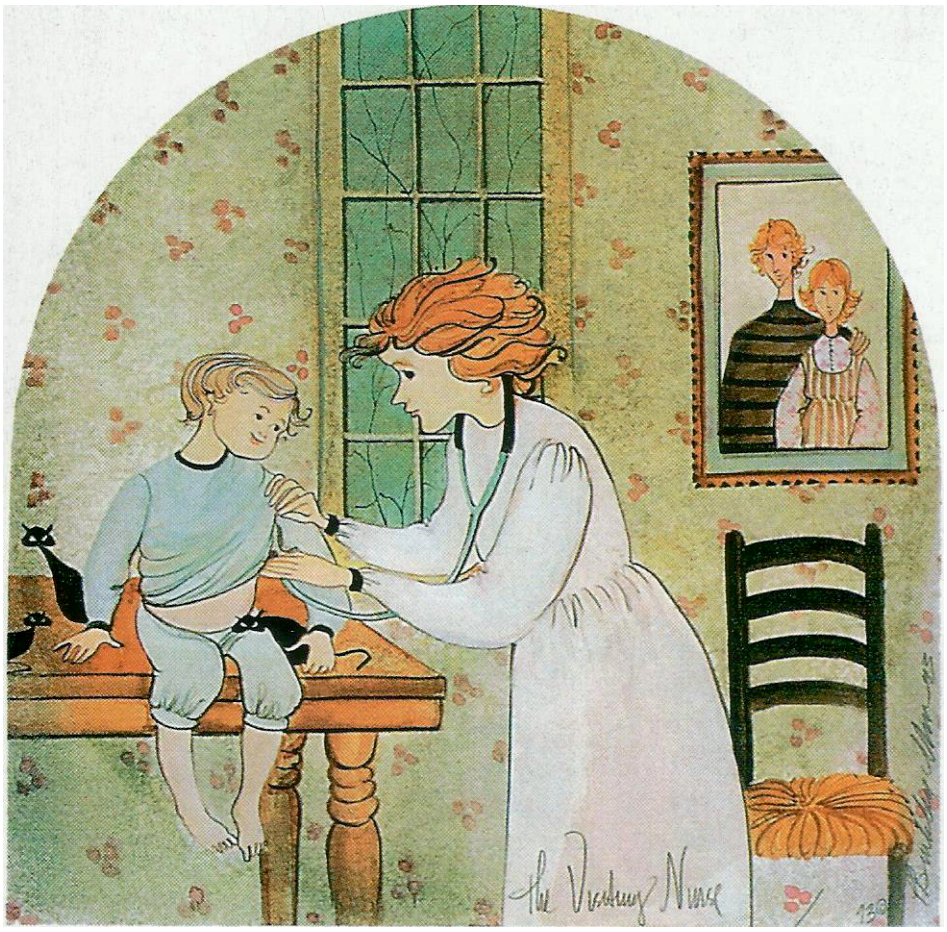

*P. Buckley Moss, "The visiting nurse", 1993, Lithography.*